Identification of anthropogenic and natural inputs of sulfate into a karstic coastal groundwater system in northeast China: Evidence from major ions, $\delta^{13}C_{DIC}$ and $\delta^{34}S_{SO4}$

Han Dongmei[a,*], Song Xianfang[a], Matthew J. Currell[b]

[a] Key Laboratory of Water Cycle & Related Land Surface Processes, Institute of Geographic Sciences and Natural Resources Research, Chinese Academy of Sciences, Beijing, 100101, China

[b] School of Civil, Environmental and Chemical Engineering, RMIT University, Melbourne, Victoria 3001, Australia

*Corresponding author: Dr. Dongmei Han

Key Laboratory of Water Cycle & Related Land Surface Processes

Institute of Geographic Sciences and Natural Resources Research

Chinese Academy of Sciences

Beijing, 100101, P.R. China

Tel: +86-10-64889367

E-mail: handm@igsnrr.ac.cn, or dmeihan@gmail.com

Abstract

The hydrogeochemical processes controlling groundwater evolution in the Daweijia area of Dalian, northeast China, were characterized using hydrochemistry and isotopes of carbon and sulfur ($\delta^{13}C_{DIC}$ and $\delta^{34}S_{SO4}$). The aim was to distinguish anthropogenic impacts as distinct from natural processes, with a particular focus on sulfate, which is found at elevated levels (range: 54.4 to 368.8 mg/L; mean: 174.4 mg/L) in fresh and brackish groundwater. The current investigation reveals minor seawater intrusion impact (not exceeding 5% of overall solute load), in contrast with extensive impacts observed in 1982 during the height of intensive abstraction. This indicates that measures to restrict groundwater abstraction have been effective. However, hydrochemical facies analysis shows that the groundwater remains in a state of ongoing hydrochemical evolution (towards Ca-Cl type water) and quality degradation (increasing nitrate and sulphate concentrations). The wide range of NO_3 concentrations (74.7-579 mg/L) in the Quaternary aquifer indicates considerable input of fertilizers and/or leakage from septic systems. Both $\delta^{13}C$ (-14.5 ‰ ~ -5.9 ‰) and $\delta^{34}S_{SO4}$ (+5.4 ~ +13.1‰) values in groundwater show increasing trends along groundwater flow paths. While carbonate minerals may contribute to increasing $\delta^{13}C_{DIC}$ and $\delta^{34}S_{SO4}$ values in deep karstic groundwater, high loads of agricultural fertilizers reaching the aquifer via irrigation return flow are likely the main source of the dissolved sulfate in Quaternary groundwater, as shown by distinctive isotopic ratios and a lack of evidence for other sources in the major ion chemistry. According to isotope mass balance calculations, the fertilizer contribution to overall sulfate has reached an average of 62.1% in the Quaternary aquifer, which has a strong hydraulic connection to the underlying carbonate aquifer. The results point to an alarming level of impact from the local intensive agriculture on the groundwater system, a widespread problem throughout China.

Keywords: groundwater, carbonate aquifer, seawater intrusion, anthropogenic pollution

1. Introduction

Degradation of groundwater quality, including salinization has become an increasingly serious global problem in coastal aquifers worldwide in recent years. With rapid economic development, population growth and increasing demand for fresh water resources, extensive groundwater withdrawals in these areas have led to water level declines and increasing groundwater salinization (e.g. Barlow and Reichard, 2010; Han et al., 2015). Many previous studies have investigated the mechanisms of salinization and potential sources of groundwater salinity in coastal aquifers, which can include evaporite mineral dissolution (e.g. Cardenal et al., 1994; Najib et al., 2016), downward/upward saline groundwater seepage (e.g., Guo et al., 1995; de Louw et al., 2013), brine migration (e.g., Han et al., 2011; Myshakin et al., 2015), and mixing caused by poorly constructed wells (e.g., Aunay et al., 2006), as well as 'classic' seawater intrusion (e.g., Daniele et al., 2013).

Coastal areas are often sites of intensive human activity, including urbanisation and agriculture. Intensive agriculture is known to be associated in some areas with salinization (e.g. Ghassemi et al, 1995; Kumar et al., 2015) and other groundwater quality issues such as addition of nitrate, sulphate and other compounds contained in fertilizers (e.g. Kaown et al, 2009; Currell et al, 2010). Environmental tracers, such as stable sulfur and carbon isotopes, e.g. $\delta^{34}S$ of dissolved SO_4 ($\delta^{34}S_{SO4}$), and $\delta^{13}C$ in dissolved inorganic carbon ($\delta^{13}C_{DIC}$), and major ion chemistry have been useful in identifying sources of salinity and dissolved sulphate

and carbonate species in groundwater (Sánchez-Martos et al., 2002; de Montety et al., 2008; Schiavo et al., 2009; Ghiglieri et al., 2012; Kim et al., 2015) and for determining water-rock interaction processes in carbonate aquifers (e.g., carbonate mineral dissolution/precipitation, cation-exchange) (Back et al., 1979; Plummer and Sprinkle, 2001; Moral et al., 2008; Daniele et al., 2013). However, to date few areas of major anthropogenic activity and known active or previous salinization from seawater intrusion have been assessed using these tracers, in order to distinguish different water quality degradation processes, such as seawater-freshwater mixing versus input of agricultural chemicals and irrigation return flow.

This study focuses on the coastal carbonate aquifers around Daweijia well field, which located in the Daweijia area of Dalian City, northeast China. Most previous investigations in this area have focused on the mechanism of seawater intrusion and related water-rock interactions (Wu et al., 1994; Yang, 2011; Zhao et al., 2012), but have ignored the potential impact of anthropogenic contributions to groundwater salinity and water quality degradation. Little is known about the influence of agricultural practices on sulphur cycling and transport in this and other coastal aquifers impacted by intensive agriculture. Here, we report new data for C and S isotopes and major ions in groundwater from the Daweijia area, which gives new insight into sources of water quality degradation, including agriculture. Using chemical and isotopic tracers, this study reveals the dominant factors controlling on groundwater hydrochemistry before and after groundwater pumping in the Daweijia well field, and

identifies the different sources of sulfate, salinity and determines the major controls on hydrochemical evolution. Understanding these issues can help to prevent further deterioration of groundwater quality in this and other similar systems in north China and elsewhere around the world.

2. Study area

The investigated area ($39^{o}10'\sim39^{o}14'$ N and $121^{o}37'\sim121^{o}45'$ E) is located in northeast China along the Bohai-Sea coast (Fig. 1). It has a catchment area of 66 km^2 to the north of Dalian City (population 3.25 million), Liaoning Province. The climate is warm temperate continental monsoon, with annual average temperature of ~10^{o}C. Most of the precipitation, totalling ~600 mm annually (Dalian Municipal Meteorological Bureau, 2014) falls during the June-September rainy season. The ephemeral Daweijia River runs through the region from east to west. Under natural conditions, groundwater discharged into the sea from the southeast towards the northwest (Fan, 1984).

The geology of the Daweijia area consists of Quaternary deposits over-lying carbonate aquifers of Paleozoic (Ordovician and Cambrian) and Proterozoic (Sinian) age. Two groups of faults are developed in this area, namely NE normal faults (F1 and F2 in Fig. 1) and EW reverse faults (F3 and F4 in Fig. 1). These structural faults cut the bedrock and are the main channel for groundwater infiltration and movement, affecting the degree of subsurface karst development (Song, 2013). The main karst development sections in the Cambrian and

Ordovician formation include (i) 5 to 20 m.a.s.l (meters above sea level) (near surface karst), (ii) -5 to -40 m.a.s.l (shallow karst), (iii) -50 to -85 m.a.s.l (medium depth karst), and (iv) < -90 m.a.s.l. (deep karst) (Zhao, 1991). The aquifers within the Daweijia area can be divided into upper and lower aquifer systems; the upper aquifer is composed of Quaternary sediments with variable thickness of 0-40 m. This consists of gravel, sand and clay layers and is not extensively pumped for water supply. The carbonate aquifers underlying the Quaternary deposits are mainly composed of Lower Ordovician, Middle and Upper Cambrian limestone, with major karst development in the medium section between -40 and -70 m.a.s.l (Lü et al., 1981; Zhao, 1991). The most productive carbonate aquifers are distributed along Daweijia River valley. Figures 1 and 2 show a geological map and stratigraphic cross-section of the hydrogeological system along this valley, showing natural groundwater flow from east to west (Fan, 1984). The geologic contacts and hydraulic connections between the upper and lower aquifer systems used in this study were determined from geologic logs and geophysical exploration during a previous investigation of regional hydrogeology in the Daweijia area (Lü et al., 1981; Jin and Wu, 1990).

Seawater intrusion was first discovered in the Dalian area in 1964. This study focuses on the coastal aquifers around Daweijia well field (Fig. 1), which was established in 1969 and formerly provided major water supply for Dalian City as the pumping rates of $12 \sim 24\times10^3$ m^3/d in 1970 (Lü et al., 1981). With the increase of pumping rate till 1983 (up to $4.8\sim6.2\times10^3$

121 m^3/d in 1977), the average chloride concentration of groundwater from eight fixed
122 monitoring wells increased from 380 mg/L in 1968 to 1137 mg/L in 1982 (Song, 2013),
123 indicating the serious seawater intrusion occurred. The groundwater withdrawal of the
124 Daweijia well field was changed from a perennial pattern to a seasonal regime with a
125 decrease by two-thirds of the pumped volume. The abstraction increased after 1991 but was
126 reduced again from 20 $\times 10^3$ m^3/d in 1995 to 4×10^3 m^3/d in 2000 (Li et al., 2006).
127 Alternatively, in order to reduce the threat of seawater intrusion to the aquifer, with the
128 establishment of surface water supply projects, water supply for Dalian City from the well
129 field has ceased since 2001, with seasonal pumping for local agricultural irrigation (Song,
130 2013). The area is also the site of ongoing intensive agricultural activity.

131 The carbonate aquifer is pumped for agricultural and public water supply. The Daweijia
132 well field was established in 1969 for water supply to Dalian City and at peak usage, the
133 upper aquifer suffered extensive drawdown. Along with this, the average chloride
134 concentration in groundwater increased from 199 mg/L in 1966 to 559 mg/L in 1991, and
135 reached a peak of 940 mg/L in 1994. Under the restrictions on groundwater extraction
136 enacted, the Cl value returned to 454 mg/L in 2005. This included the drastic measure of
137 switching off the well field supplying Dalian City since 2001 (Song, 2013). Although the
138 groundwater levels have recovered in recent years, groundwater salinity has not completely
139 been reversed, and elevated nitrate and sulphate concentrations have continued since this time.

140 Potential causes include 'residual' seawater intrusion which has not yet re-equilibrated with
141 recovered water levels and/or different sources of contamination, associated with agriculture
142 or urban activities.

143 **3. Methods**

144 **3.1 Sampling and analysis**

145 We collected 30 water samples during two sampling campaigns (June 2006 and August
146 2010) for analysis of major ions and stable isotopes ($\delta^{13}C_{DIC}$ and $\delta^{34}S_{SO4}$). The samples
147 include 29 from wells and one seawater sample. Sampling wells are production wells with
148 variable depths (8.4-128 m) and screened intervals (lengths of 2-35 m, see Table 1) and these
149 are distributed mainly along the Daweijia River valley (Fig. 1). The screened intervals of
150 wells in the carbonate aquifer are mainly between 65-100 m below ground surface (Table 1).
151 Before sampling, the wells were pumped for at least for half an hour until physico-chemical
152 parameters (e.g., water temperature, pH, electrical conductivity and dissolved oxygen)
153 stabilised. All samples were filtered through 0.45μm pore-size filter paper and stored in
154 HDPE bottles at 4^{o}C in a cool room until analysis. The samples prepared for cation analysis
155 were acidified to pH<2 by adding high purity HNO_3. Bicarbonate was determined in the field
156 by titrating with 0.22N H_2SO_4. Major anions were measured by ion chromatography
157 (SHIMADZU), and major cations were determined using ICP-AES by the Laboratory of
158 Physics and Chemistry, Institute of Geographic Sciences and Natural Resources Research

159 (IGSNRR), Chinese Academy of Sciences (CAS). The ion balance errors of the chemical
160 analyses were generally within ±15%. The hydrogeochemical code PHREEQC-2 (version
161 2.18.3, Parkhurst and Appelo, 1999) was used to determine the saturation indexes (SI) of
162 calcite, dolomite and gypsum.

163 The $\delta^{13}C$ values of dissolved inorganic carbon (DIC) in 16 water samples were
164 measured using continuous flow on a Finnigan MAT 252 mass spectrometer, with the
165 automated headspace analysis of the preparation device, in the State Key Laboratory of
166 Environmental Geochemistry, Institute of Geochemistry (Guiyang), CAS. The results of $\delta^{13}C$
167 analysis are expressed in conventional delta (δ) notation, defined as $\delta = (R_{sample} -$
168 $R_{standard})/R_{standard} \times 1000$, where R is the ratio of $^{13}C/^{12}C$. The $\delta^{13}C$ values of dissolved
169 inorganic carbon (DIC) are expressed relative to the standard Vienna Peedee Belemnite
170 (VPDB), with an analytical precision of ±0.2‰. Samples for ^{34}S in dissolved sulfate in 18
171 groundwater samples (Table 1) were measuredby a Finnigan MAT Delta-S gas mass
172 spectrometer after on-line pyrolysis with an EA (Elemental Analyzer) in the Laboratory for
173 Stable Isotope Geochemistry, Institute of Geology and Geographysics, CAS. The method of
174 Halas and Szaran (1999) was used for converting precipitated $BaSO_4$ to SO_2. The
175 international standard against which $\delta^{34}S$ values are referenced is the troilite (FeS) phase of
176 the Cañon Diablo meteorite (CDT), which has a $^{34}S/^{32}S$ abundance ratio of 0.0450 and are

reported as δ (‰) difference from the standard with an analytical precision of better than or about ±0.4‰.

3.2 Ionic deltas and mixing calculations

To further investigate the hydrochemical behaviour of major cations and diagnose the processes modifying hydrochemical composition of groundwater in the aquifer, ionic delta values were calculated. The delta values express enrichment or depletion of particular ions relative to a conservative mixing system. These have been used in previous studies as effective indicators of groundwater undergoing freshening or salinization, along with associated water-rock interaction processes (primarily cation exchange – e.g., Appelo, 1994). Based on variations of molar Cl/Br ratios and major ions in groundwater (section 5.1), we have ruled out significant sources of Cl^- other than meteoric and oceanic inputs. It is assumed in these calculations that there is no chloride input from salts in the aquifer matrix itself, and that Cl can be regarded as the most conservative species during mixing and hydrochemical evolution. The fraction of seawater (f_{sea}) in a groundwater sample can thus be calculated using (Appelo and Postma, 2005):

$$f_{sw} = \frac{C_{Cl,sam} - C_{Cl,f}}{C_{Cl,sw} - C_{Cl,f}} \quad (1)$$

where $C_{Cl,sam}$, $C_{Cl,fresh}$, and $C_{Cl,sw}$ refer to the Cl concentration in the sample, freshwater, and seawater, respectively.

195 The theoretical concentration ($C_{i,mix}$) of an ion i in a water sample can be calculated by
196 comparing the measured concentration of this ion with its expected composition from
197 conservative mixing between seawater and freshwater (Appelo and Postma, 2005):

198 $$C_{i,mix} = f_{sw} \cdot C_{i,sw} + (1 - f_{sw}) \cdot C_{i,f} \quad (2)$$

199 where $C_{i,sam}$ and $C_{i,f}$ -the measured concentration of the ion i in the water sample and
200 freshwater, respectively; f_{sw}- fraction of seawater. The ionic deltas (ΔC_i) of ion i can thus be
201 obtained by:

202 $$\Delta C_i = C_{i,sam} - C_{i,mix} \quad (3)$$

203 **4. Results**

204 **4.1 Chemical analysis**

205 The physical and chemical characteristics of groundwater samples from the Quaternary
206 aquifer (QA) and the Cambrian-Ordovician carbonate aquifer (COA) in the Daweijia are
207 compiled in Table 1. Total dissolved solids (TDS) concentrations vary from 372 to 2403
208 mg/L, with values increasing along the main direction of groundwater flow from the east
209 towards the sea. Groundwater pH ranges from 6.5 to 7.6 with a mean of 7.2. Dissolved
210 oxygen concentrations range from 1.3 to 8.6 mg/L with a mean of 5.6 mg/L. The fresh (<1
211 g/L TDS) groundwater (e.g., CG6, CG14) is characterized as Ca-HCO_3(·Cl) type water,
212 while brackish (1 to 10g/L TDS) groundwater (e.g., CG7, CG10, CG11, CG17) is
213 predominantly Ca-Cl type in the carbonate aquifer. Brackish groundwater in the shallow

214 Quaternary aquifer was observed to be Ca-Cl·SO_4 type water, or near the coastline, (e.g.,
215 QG10, QG11) Na·Ca-Cl(·HCO_3) type.

216 According to mixing calculations, minor seawater intrusion near the coastline is
217 identified (Fig. 3), however the fraction of seawater does not exceed 5% and this compares
218 with a fraction of 20.8% observed in 1982 (Wu et al., 1994). The groundwater in this study is
219 characterized by a wide range of sulfate concentrations between 54.4 and 368.8 mg/L, with a
220 mean value of 174.4 mg/L. Nitrate concentrations ranged from 43.1 to 579.4 mg/L with a
221 mean value of 206.9 mg/L, far beyond the drinking water standard (50 mg/L) in China. The
222 investigated seawater sample also has a very high nitrate concentration of 1092 mg/L.

223 Comparing background data (1962, Lü et al., 1981) and current data (2010, in this study),
224 the nitrate concentrations in groundwater increased from a range of 0~10.9 mg/L (n=51,
225 mean value of 2.1 mg/L) in 1962 to a range of 43.1~579.4 mg/L (n=15, mean value of 207.1
226 mg/L) in 2010 in the carbonate aquifer, and mean sulfate concentration increased from a
227 range of 0~121.6 mg/L (n=64, mean value of 72.4 mg/L) in 1962 to a range of 65.1 ~ 306.9
228 mg/L (n=15, mean value of 154.1 mg/L) in 2010. For the Quaternary aquifer, nitrate
229 concentrations have changed from a range of 0~9.9 mg/L (n=3, mean value of 6.7 mg/L) in
230 1962 to a range of 74.7 ~ 347.9 mg/L (n=9, mean value of 199.2 mg/L) in 2010, and sulfate
231 from a range of 0~64.1 mg/L (n=3, mean value of 35.2 mg/L) in 1962 to a range of 54.4 ~
232 368.8 mg/L (n= 9, mean value of 224.1 mg/L) in 2010.

233 The ionic delta values are plotted in Fig. 3, illustrating the varied distribution of
234 geochemical types and evolution in the aquifer. Generally most groundwater samples are
235 characterized by negative ΔNa^+ values and positive ΔCa^{2+} values. Some brackish
236 groundwater samples have negative ΔNa^+ values and positive ΔCa^{2+} + ΔMg^{2+} values,
237 displaying a deficit of Na^+ with a corresponding excess in Ca^{2+} and Mg^{2+}. There are positive
238 values of ΔSO_4^{2-} observed in most groundwater sample, and these are particularly high in the
239 brackish groundwater (Fig. 3d).

240 **4.2 Dissolved inorganic carbon (DIC) and $\delta^{13}C_{DIC}$**

241 Fig. 4 presents the $\delta^{13}C_{DIC}$ isotope data and this can be used to infer the sources and
242 evolution of dissolved inorganic carbon in the investigated groundwater (Clark and Fritz,
243 1997). The measured $\delta^{13}C_{DIC}$ values in groundwater range from -14.5 ‰ to -5.9 ‰ vs. PDB,
244 with a mean value of -10.5 ‰ (Table 1). The water samples from the carbonate aquifer show
245 a relatively narrow range of $\delta^{13}C_{DIC}$ values (-12 to -8.4 ‰ with a mean value of -10.1 ‰, n=8)
246 comparable to the range of $\delta^{13}C_{DIC}$ values (-14.5 to -5.9 ‰, mean of -10.0 ‰, n=7) from the
247 Quaternary aquifer. The waters collected in the upstream areas show $\delta^{13}C$ values from -14.5
248 to -12.8 ‰, while the middle area has values of -12.0 to -9.0 ‰ and the coastline values
249 between -10.6 to -5.9 ‰ (Fig. 4, Table 1).

250 The local seawater sample (SW1) has a $\delta^{13}C_{DIC}$ value of -3.3‰, which is relatively low
251 compared to other reported values of modern seawater (-1~+2 ‰, Clark and Fritz, 1997).

252 Carbon in C_4 plants, which include maize, sugar cane and sorghum, has $\delta^{13}C$ values that
253 range from -10 to -16 ‰ with a mean value of ~ -12.5 ‰, while most C_3 plants have $\delta^{13}C$
254 values that range from -24 to -30 ‰ with an average of ~ -27 ‰ (Vogel, 1993). Maize is the
255 main agricultural product in the study area (Hu, 2010), indicating a C_4 vegetation source may
256 be dominant. Carbonate dissolution and/or exchange leads to progressive enrichment of $\delta^{13}C$
257 values towards the values of the mineral, usually with values between -2 and +2‰.

258 **4.3 Stable isotopes of sulfate**

259 The $\delta^{34}S_{SO4}$ compositions varied between +5.4 and +13.1‰ (Table 1). Sample CG1, with
260 a sampling depth of 100 m and collected from the centre of a residential area, has the highest
261 $\delta^{34}S_{SO4}$ value (+13.1‰). The lowest $\delta^{34}S_{SO4}$ value (+5.4 ‰) was found for sample QG3
262 collected in an upstream area. Water samples from the carbonate aquifer are denoted with
263 dashed line in Fig. 5 and have relatively high $\delta^{34}S_{SO4}$ values (ranging from +6.6 to +13.1 ‰
264 with mean value of +9.9 ‰, n=9) and low SO_4/Cl ratios. The groundwater samples from the
265 Quaternary aquifer are characterized by a relatively narrow range of $\delta^{34}S_{SO4}$ values (ranging
266 from +5.4 to +10.1 ‰ with mean value of +7.9 ‰, n=8) and wider range of SO_4/Cl ratios.
267 Some brackish groundwater (QG2 and QG10) from the Quaternary aquifer also shows these
268 characteristics (Fig. 5). In general, the $\delta^{34}S_{SO4}$ values increase with correspondingly lower
269 SO_4/Cl ratios in the direction of the coastline.

5. Discussion

A number of geochemical processes control the evolution of groundwater in the study area. Some of these processes show evidence of taking place in both carbonate and Quaternary aquifers, while others are more confined to one of the aquifers. The major hydrochemical processes inferred from the data are summarized in Table 2, which also includes a description of lines of evidence used to infer these (in most cases 2 supporting lines of evidence exist).

5.1 Seawater intrusion, freshening and cation exchange

Widespread seawater intrusion appears to be a thing of the past, although local salinization continues around the well field. Chloride is an important index for estimating the extent of seawater intrusion, and is generally assumed to behave relatively conservatively. The molar Cl/Br ratios (based on values from this study and Yang et al, 2011) range from 118.3 to 633.1 (n=11, mean value 394.3), which is generally below the oceanic ratio of ~650 (Drever, 1997). As halite is Br-depleted from its mineral structure, halite precipitation may lead to depletion of the ratios, however it is unlikely that saturation with respect to halite could be reached in the groundwater (e.g., McCaffrey et al., 1987; Edmunds, 1996; Cartwright et al., 2004). Minor contamination, e.g., with pesticides such as ethyl dibromine, methyl bromide and/or preferential Cl adsorption on organic material may explain the lower than usual ratios. Overall the ratios do not indicate significant sources of additional Cl. The

289 TDS concentrations of groundwater in this study area varied within a range of 0.4-4.5 g/L in
290 1981 (the peak period of seawater intrusion) (Lü et al., 1981). For the well CG2 located in the
291 centre of the well field, TDS was 0.3 g/L on December 1965, 0.71 g/L on August 1981, 0.66
292 g/L on December 1981, and up to 1.19 g/L on August 2010, an obvious increasing trend,
293 however, Cl^- concentrations decreased from 375.6 mg/L in August 1981 to 288.4 mg/L in
294 August 2010.. By contrast, there are much more significant increases on SO_4^{2-} and NO_3^-
295 concentrations in groundwater, which explains increasing TDS but decreasing chloride. For
296 the well CG2, SO_4^{2-} concentration increased 5 times from 38.2 mg/L in August 1981 to 189.2
297 mg/L in August 2010. While NO_3^- concentration increased 4 times from 64.6 mg/L in August
298 1981 to 263.9 mg/L in August 2010 – far higher than the overall changes in TDS. These
299 changes of different ions concentration in groundwater show that the anthropogenic input
300 (e.g., application of agricultural fertilizer) has modified the hydrochemical composition of
301 groundwater to great extent after the cessation of pumping in the well field.

302 The freshening of coastal aquifers can be shown using the multi-rectangular HFE-
303 diagram (Fig. 6). This classification method proposed by Giménez-Forcada (2010) can be
304 employed to determine the dynamics of seawater intrusion, considering the percentages of
305 major ions, showing the intruding and freshening phases in hydrochemical facies evolution.
306 The fresh water in the recharge area mainly belongs to the Ca-MixHCO_3 (14) facies, and
307 seawater belongs to the Na-Cl (4) facies. Most of the groundwater samples don't follow the

308 predicted succession of facies along the mixing line (4-7-10-13), and rather indicate a small
309 degree of simple mixing between fresh and seawater components, along with inverse cationic
310 exchange between Na and Ca. This leads to the water reaching the Ca-Cl (16) facies observed
311 in brackish groundwater in the carbonate aquifer. The surplus Ca^{2+} from ion exchange may
312 also cause super-saturation with respect to calcite and dolomite; consistent with the observed
313 positive values in the majority of samples (Langmuir, 1971). Net dissolution of carbonate
314 minerals is not evident as a major process in the groundwater, as is shown by a number of
315 lines of evidence below (Mg/Ca ratios, stable isotopes of DIC – see Table 2). Cation
316 exchange is thus considered crucial to the development of the Ca-Cl facies in the more
317 evolved waters.

318 Generally most groundwater samples collected from the west of Daweijia well field are
319 characterized by depletion of Na^+ more or less balanced by equivalent enrichment of Mg^{2+}
320 plus Ca^{2+}. Both ΔNa^+ and ΔMg^{2+}decrease with an increasing fraction of seawater (f_{sw}),
321 especially for f_{sw} > 3% (Fig. 3), which would be more characteristic of a salinization-driven
322 base exchange process (Appelo and Postma, 2005). This may suggest a residual effect from
323 the previous saline intrusion which is yet to re-equilibrate with the aquifer matrix. Most
324 groundwater samples from the carbonate aquifer show ΔCa^{2+}, ΔMg^{2+}, and ΔSO_4^{2-} increases
325 with salinity whereas ΔNa^+ decreases as salinity increases (Fig. 3), consistent with inverse
326 cation exchange.

For fresh groundwater in the carbonate aquifer, the ionic deltas values are close to 0, indicating the modifying processes are controlled by conservative mixing and there has been little chemical interaction between the groundwater and the aquifer material. Compared to the conservative mixing, the excess of SO_4 observed (positive ΔSO_4^{2-} values) might be attributed to gypsum dissolution, under the influence of seawater intrusion (creating temporary under-saturation). However, only greater degrees of seawater intrusion can cause gypsum dissolution to result in the SO_4 excess (Daniele et al., 2013), and the chloride data are inconsistent with ongoing seawater intrusion. It can therefore be inferred that there must be an additional source of SO_4. Anthropogenic fertilizer input may explain the increases in SO_4^{2-} along with NO_3^- and possibly even Ca^{2+} and Cl^- in the aquifer, as is discussed further below.

5.2 Groundwater interaction with carbonate minerals

The evolution of DIC and $\delta^{13}C_{DIC}$ in the carbonate system begins with atmospheric CO_2 with $\delta^{13}C$ value ~ -7‰ VPDB, while subsequent dissolution of soil gas carbon dioxide leads to depletion of the carbon depending which source of vegetation is dominant (Clark and Fritz, 1997). Concentrations of DIC in fresh and brackish groundwater were in the range of 60.1-446.5 mg/L (average 189.2 mg/L) and 46.2 - 512.7 mg/L (average 203.1 mg/L), respectively (Table 1). The $\delta^{13}C_{DIC}$ values of groundwater ranging from -14.5 ‰ to -5.9 ‰ vs. PDB are similar to groundwater from carbonate aquifers in southwest China, which has typical values, ranging from -15.0 ‰ to -8.0 ‰ (Li et al., 2010). The $\delta^{13}C_{DIC}$ in groundwater shows a

346 negative correlation with DIC concentration, particularly in the karst aquifer (Fig. 4). This
347 indicates that simple, congruent dissolution of carbonate minerals is not a major source of
348 DIC in the groundwater. Rather, $\delta^{13}C_{DIC}$ may undergo progressive equilibration with aquifer
349 carbonate during sequential carbonate dissolution/precipitation reactions (e.g. de-
350 dolomitization). This is consistent with the increasing Mg/Ca ratios observed along the flow
351 path, along with increasing $\delta^{13}C_{DIC}$ values in the carbonate aquifer (see Fig. 7a), but no
352 overall increase in HCO_3 (Fig. 4 and Table 2). Near the coastline, the more enriched $\delta^{13}C_{DIC}$
353 values and lower DIC may also result due to mixing with seawater. An increasing trend in
354 SO_4 and Mg concentrations and Mg/Ca ratios along the flow path are also indicative of de-
355 dolomitization (e.g. Jones et al., 1989; Plummer et al., 1990; López-Chicano et al., 2001;
356 Szynkiewicz et al., 2012) in which the dissolution of gypsum and anhydrite lead to over-
357 saturation and thus dolomite dissolution and calcite precipitation. For deeper carbonate
358 groundwater underlying the Daweijia wellfield, the negative correlation between Ca^{2+} and
359 $\delta^{13}C_{DIC}$ (Fig. 7b) also indicate that Ca enrichment in groundwater may be not attributed to
360 carbonate dissolution. The increase in $\delta^{13}C$ with decreasing Ca content is likely related to the
361 incongruent reaction, which removes Ca from solution and progressively increases $\delta^{13}C$ to
362 equilibrate with the aquifer matrix. In the Quaternary aquifer, the minor calcite dissolution
363 occurring could lead to increasing $\delta^{13}C$ with increasing Ca. An alternative process may
364 remove the HCO_3 along flow paths (e.g., CO_2 de-gassing).

365 Deines et al. (1974) showed that there are significant differences in the relationships
366 between carbon isotopic composition and chemical variables for open and closed system
367 conditions. Based on their model (which uses similar initial conditions to the study area) the
368 chemical and isotopic composition of groundwater at a given pH in equilibrium with a
369 reservoir of a given P_{CO2} and $\delta^{13}C_r$ can be estimated. For the closed system model the ^{13}C
370 content of the solution depends not only on the $^{13}C/^{12}C$ ratio of the reservoir CO_2 ($\delta^{13}C_r$), but
371 also on that of the dissolving carbonate rock ($\delta^{13}C_{rock}$). The pH and $\delta^{13}C$ values of the
372 carbonate aquifer groundwater suggest evolution in a relatively closed system. Lower $\delta^{13}C$
373 value (-14.5‰) of shallow groundwater (QG4) in recharge area may be more affected by the
374 soil CO_2 in areas of intensive corn cultivation, ranging from approximately -18 to -25‰
375 (Deines et al., 1974). In this area, the irrigation using local carbonate groundwater may have
376 resulted in mixing between the shallow groundwater with similar values to this, and the deep
377 water from the carbonate aquifer (with higher values), leading to the intermediate value
378 observed. Most groundwater in the study area is supersaturated with respect to calcite and
379 dolomite (Han et al., 2015). The hydrochemical composition of groundwater is influenced by
380 CO_2 exsolution and $CaCO_3$ precipitation, which can be described by the reaction:

381 $$Ca^{2+} + 2HCO_3^- = CaCO_3\downarrow + CO_2(g)\uparrow + H_2O$$

382 At isotopic equilibrium CO_2 is enriched in ^{12}C and $CaCO_3$ in ^{13}C with respect to HCO_3^-
383 (Deines et al., 1974). Since for each mole of CO_2 exsolved one mole of $CaCO_3$ is precipitated,
384 the kinetic isotope effects is removal of ^{12}C enriched carbon from the solution, which

385 concentrates ^{13}C in the remaining HCO_3^-. The enrichment of $\delta^{13}C_{DIC}$ without change in
386 HCO_3^- content may thus be caused by $^{12}CO_2$ loss during exsolution and ^{13}C enrichment in
387 solution. Dolomite dissolution is likely to add Ca^{2+}, Mg^{2+}, and HCO_3^- to the solution, while
388 calcite precipitation will remove DIC and retain calcite saturation, resulting in generally
389 increasing Mg/Ca ratios along flow paths, along with increasing $\delta^{13}C$ values (Freeze and
390 Cherry, 1979; Edmunds et al., 1987; Cardenal et al., 1994; Kloppmann et al., 1998). The
391 dissolution of even very small amounts of gypsum may cause this process to occur in
392 carbonate aquifers, which usually characterized by near saturation with respect to calcite, by
393 creating temporary under-saturation (due to the addition of calcium but not bicarbonate ion)
394 (Plummer et al., 1990; López-Chicano et al., 2001; Moral et al., 2008; Szynkiewicz et al.,
395 2012).

396 Additionally, Sr is good proxy for Ca variations and sources with higher correlation, and
397 the concentration of Sr^{2+} is often particularly high and frequently correlated with SO_4^{2-}
398 concentrations (Figure 8). In addition to Sr's origin from celestite, which may be present as
399 microcrystalline inclusions in gypsum, Sr^{2+} can also occur as solid solution in carbonate
400 minerals (Hunkeler and Mudry, 2007). Large amounts of anthropogenic chemical input will
401 change these highly correlated relationships. Fig. 8 shows different slopes in the relationship
402 between Cl/TDS and Sr for different water types. The chloride-rich brackish water with high
403 Cl/TDS ratios has high Sr contents in the carbonate aquifer; in contrast, the sulphate-rich

404 brackish water with low Cl/TDS has wide range of Sr contents in the Quaternary aquifer. The
405 higher Sr contents in the COA likely result due to enhanced from water-rock interaction
406 (carbonate minerals dissolution), possibly enhanced by historic seawater intrusion.

407 Another possible control on the carbon chemistry of the groundwater is that active re-
408 circulation of water is taking place in the unsaturated zone of the aquifer due to
409 anthropogenic activity. In the local agricultural soils, CO_2 concentration is usually high, with
410 a $\delta^{13}C_{DIC}$ between -6.3 and -13.1‰ and $\delta^{13}C$ of dissolved organic carbon between -23.2 and -
411 21.8 ‰ (Yang, 2011). During recharge events, water dissolves the soil CO_2 which is involved
412 in carbonate dissolution and becomes part of the DIC pool. If this process is conducted over
413 successive irrigation, the HCO_3^- concentration increases and $\delta^{13}C_{DIC}$ will deplete owing to the
414 dissolved biogenic CO_2 in soil.

415 **5.3 Sources of dissolved SO_4 to groundwater**

416 Dissolved SO_4^{2-} of groundwater in the coastal aquifers might originate from several
417 sources, potentially including (i) natural and artificial sulfates in rainwater; (ii) dissolution of
418 sulphate-bearing evaporates (e.g. gypsum and anhydrite); (iii) seawater; (iv) anthropogenic
419 pollutants (e.g. domestic sewage, detergent and agricultural fertilizers). The $\delta^{34}S$ of
420 groundwater SO_4 are used as a tracer to identify the sources of dissolved SO_4^{2-} to the
421 groundwater in this study. Fig. 5 shows the relation between $\delta^{34}S_{SO4}$ values and SO_4/Cl for
422 groundwater samples, showing typical literature values for sulfur isotopic composition of

major sulphate sources. Most of water samples from the Daweijia area have sulfur isotopic compositions that reflect mixed sources. The $\delta^{34}S_{SO4}$ values are generally lower in the upstream area (+5.4~ +5.7 ‰) increasing along the groundwater flow paths towards the coast (+13.1‰). Enrichment in $\delta^{34}S_{SO4}$ may result from sulphate reduction, whereas sulphide oxidation generally leads to negative $\delta^{34}S_{SO4}$ values (Clark and Fritz, 1997). However, there are no negative $\delta^{34}S_{SO4}$ values observed in this study area, indicating minor or negligible sulphide (such as pyrite) oxidation occurring in the aquifer.

$\delta^{34}S_{SO4}$ value of modern seawater is approximately +21‰ (Rees et al., 1978). The $\delta^{34}S_{SO4}$ of groundwaters, ranging from +13.1 to +5.4 ‰ with a mean value of +8.9 ‰, thus generally discount this as a significant source of sulphate, consistent with the low mixing fractions calculated using Cl. The $\delta^{34}S_{SO4}$ values of precipitation from 8 stations in the north region of Yangtze River ranges from +4.9 % to +11.0 ‰ (Hong et al., 1994). Aside from CG1, the $\delta^{34}S_{SO4}$ compositions of the samples overlap with the isotopic range of rainfall. However, rainfall is characterized by higher SO_4/Cl (2.26, Zhang et al., 2012) than the groundwater (0.16~0.97) and significantly lower total concentrations than are observed; indicating that this is only a partial origin of sulfate in groundwater. Sulfate minerals (gypsum, anhydrite, etc.) from marine sources typically have $\delta^{34}S_{SO4}$ values between +9 and +30.2‰ (Shi et al., 2004; Vitòria et al., 2004). As groundwater flows downwards into the deeper karst aquifer, the $\delta^{34}S$ values increase and approach the values in marine evaporites,

part of the continuous de-dolomitization reaction discussed above. However, this can't explain the observed sulfate levels in the Quaternary aquifer (see mass balance calculations below).

Fertilizers have a wide range of $\delta^{34}S_{SO4}$ values ranging from -6.5 to +11.7 ‰, with a mean value of +3.7 ‰ and -0.8 ‰ in the northern hemisphere (Szynkiewicz et al., 2011) and China (Li et al., 2006), respectively. Apart from CG1 ($\delta^{34}S_{SO4}$ value of +13.1‰), the $\delta^{34}S_{SO4}$ values of the rest groundwater samples are within the $\delta^{34}S_{SO4}$ ranges of known fertilizers. The isotopic $\delta^{34}S$ values in fertilizers significantly differ from the geological SO_4 inputs of sedimentary origin, and over-lap with most of the observed compositions (Fig. 5). In addition the very high nitrate concentrations observed in the groundwater (up to 625 mg/L) strongly indicate a high input of excess fertilizer residue via irrigation returns to the aquifer. This indicates that sulfate in fertilizers should be taken into account as a major contributing source of dissolved SO_4 in groundwater, especially from the Quaternary aquifer. This is also confirmed by the general positive relationship between NO_3^- and SO_4^{2-} concentrations (Fig. 9a) and correlation (albeit weak) between $\delta^{34}S$ values and NO_3 concentrations in the Quaternary aquifer (Fig. 9b). It can be assumed that other anthropogenic sources of SO_4 such as atmospheric deposition or detergents from domestic/wastewater sources, or pig manure are negligible in the study area.

Despite they clear overlap in $\delta^{34}S$ of fertilizers and groundwater SO_4^{2-}, the $\delta^{34}S$ measured in upstream locations (e.g. QG3 and QG4) probably reflect inputs from geologic SO_4 sources (such as soil sulfate) (Fig. 5). In contrast, the sulfur isotope values are more consistent with marine sedimentary sources of groundwater SO_4 in the carbonate aquifer, due to the sustained water-rock interaction and longer residence time. The evidence for gypsum dissolution as part of de-dolomotization in the major ion and carbon isotope data (discussed above) is also consistent with a marine evaporite source of sulphur in the deeper aquifer.

Both $\delta^{13}C$ and $\delta^{34}S_{SO4}$ values increase along the groundwater flow path (Table 3). Groundwater with low $\delta^{13}C$ values (e.g. -14.5‰) and $\delta^{34}S_{SO4}$ values (e.g. ~+5.4‰) represents recently recharged water, which is dominated by unsaturated zone processes and diffuse flow. Equilibration with carbonate minerals in the aquifer matrix during de-dolomitization makes an important contribution to the groundwater $\delta^{13}C$ evolution in the karst aquifer ($\delta^{13}C$ up to -5.9 ‰ in QG11), reaching saturation with respect to calcite and dolomite. Then, the high loads of fertilizers accessible during agricultural return flow are the most likely source of the dissolved sulfate and nitrate, particularly in the shallow Quaternary aquifer.

5.4 Anthropogenic contribution on groundwater chemistry and environmental implications

Fertilizers are applied beyond what is taken up by crops in the long term in many parts of China (Davidson and Wei, 2012) as evident from the high NO_3^- concentrations in

groundwater. The wide range of NO_3 concentrations, indicate considerable anthropogenic input under human activities (e.g., fertilizer usage during irrigation, leakage from septic system), which is responsible for the deterioration of local groundwater and near shore sea-water quality. NO_3^- concentrations are obviously elevated (e.g. 75-386 mg/L) in the shallow groundwater from the Quaternary aquifer, especially near the Daweijia well field, resulting from agricultural fertilization. Due to nitrate input from fertilizers, the relatively low nitrate concentrations in some deep groundwater (e.g. CG4, CG14), which are located in the upstream area, show that, compared with groundwater in the downgradient area, these waters have locally reduced impacts from contamination. However, many deep groundwater samples have similar ranges of NO_3^- concentrations to shallow groundwaters, indicating that there is hydraulic connection between shallow and deep aquifers (e.g. QG5 and CG7 in Fig. 2).

To quantify the fertilizers contributions to groundwater chemistry, we considered the inputs of precipitation infiltration, seawater intrusion and evaporite dissolution into groundwater system. We used a mass balance approach to evaluate the contribution of difference sources of sulphate to the dissolved SO_4^{2-} of groundwater. The four sources of sulphate in the dissolved SO_4^{2-} of groundwater are from precipitation, seawater, fertilizer and evaporate dissolution. The isotopic composition of groundwater sulphate ($\delta^{34}S_{SO4}$) can be calculated by:

$$\delta^{34}S_{gw}\times SO_{4,gw}=\delta^{34}S_{prec}\times SO_{4,prec}+\delta^{34}S_{sw}\times SO_{4,sw}+\delta^{34}S_{fer}\times SO_{4,fer}+\delta^{34}S_{evp}\times SO_{4,evp} \quad (7)$$

where $\delta^{34}S_{prec}$, $SO_{4,prec}$, $\delta^{34}S_{sw}$, $SO_{4,sw}$, $\delta^{34}S_{fer}$, $SO_{4,fer}$, $\delta^{34}S_{evp}$, and $SO_{4,evp}$, correspond to the end member $\delta^{34}S$ values for rainfall (+5.39‰, Hong et al., 1994), seawater (+21‰, Clark and Fritz, 1997), fertilizer (-0.8 ‰, Li et al., 2006), and sulfate marine evaporates of Cambrian-Ordovician age (+28‰, Clark and Fritz, 1997). The dissolved SO_4^{2-} concentration ($SO_{4,gw}$) in groundwater is the total sulphate contribution from precipitation, seawater, fertilizer and evaporate:

$$SO_{4,gw}=SO_{4,prec}+SO_{4,sw}+SO_{4,fer}+SO_{4,evp} \quad (8)$$

$$\text{where } SO_{4,prec}=[SO_{4,prec}]\times R=8.02\text{mg/L}\times 0.783 \quad (9)$$

$$SO_{4,sw}=[SO_{4,sw}]\times f_{sw}=2710\text{mg/L}\times f_{sw} \quad (10)$$

The SO_4^{2-}concentration ($[SO_{4,prec}]$=8.02 mg/L) of the local precipitation was reported by Zhang et al., 2012, and SO_4^{2-}concentration ($[SO_{4,sw}]$=2710 mg/L) of the seawater referenced from Clark and Fritz, 1997. *R* is the recharge rate equal to the ratio of the amount of precipitation infiltration and the amount of the total groundwater resources in the study area. According to the water balance calculations in the local groundwater flow system (CGS, 2007), groundwater is mainly recharged from precipitation infiltration, which occupied 78.3% (*R*) of the total recharge water volume. f_{sw} can be calculated by the equation (1) for each groundwater sample.

515 The results of the mass balance, showing sulphate contribution to groundwater from
516 fertilizer (assuming these end-members correspond to values in the study area) are shown in
517 Fig. 10. In total, 4 to 22% of the dissolved SO_4^{2-} concentrations in groundwater are
518 contributed from evaporite dissolution, whereas 30 to 75% of the dissolved SO_4^{2-}
519 concentrations in groundwater can be ascribed to input from fertilizers. According to these
520 calculations, overall, the local application of the fertilizers is now responsible for the majority
521 of dissolved SO_4^{2-} in groundwater. The contribution reaches on average 62.1% in the
522 Quaternary aquifer and 48.7% in the deeper carbonate aquifer; showing that the shallow
523 Quaternary aquifer is particularly prone to pollution by fertilizer utilization. The sulphate
524 contributions to groundwater from seawater and precipitation are less than 10%, which is
525 relatively lower and is consistent with the observation that pumping restrictions have
526 effectively halted saline intrusion in the area. We analysed the sensitivity of the mass balance
527 by changing ±10% of the end-member sulfur isotope compositions of fertilizer and evaporate,
528 respectively. We found the change on $\delta^{34}S_{fer}$ varied the contributions from fertilizer and
529 evaporate by ± 0.1% and ± 0.2% respectively. The ±10% change in $\delta^{34}S_{evp}$ leads to changes
530 in the contributions from fertilizer and evaporate by ± 0.4% and ± 2%, respectively. This
531 suggests that the results are more sensitive to $\delta^{34}S_{evp}$ values in the mass balance.
532 Although further investigation is needed to determine the contribution of dissolved
533 sulphate from different pollution sources (the end-member values used above are naturally

534 uncertain and may bias the overall % contributions), the current results indicate that the
535 anthropogenic contaminant input plays dominant role in providing sulfate to the shallow
536 groundwater (as well as nitrate), and that this influence has extended into the deeper
537 carbonate aquifer. This widespread shift towards agricultural return flow becoming the
538 dominant control on groundwater chemistry, particularly in shallow aquifers, is consistent
539 with what is unfolding over many areas of northern China (Currell et al, 2012). This is a
540 disturbing trend, particularly given the time-lags involved in groundwater systems
541 equilibrating towards new water quality norms, which suggest significant future degradation
542 of groundwater resources will continue to occur in these areas.

543 **6. Conclusions**

544 The coastal aquifer in the Daweijia area, northeast China is composed of interlayered
545 Quaternary sedimentary and Cambrian-Ordovician carbonate rocks. The groundwater has
546 evolved from fresh water (meteoric recharge) to brackish water in series of water types:
547 Ca(·Mg)-HCO_3·Cl → Ca·Na-Cl·HCO_3 → Ca-Cl → Na·Ca-Cl→ Na-Cl via a combination of
548 natural and anthropogenic processes. After the cessation of the groundwater pumping in the
549 Daweijia well field, the TDS concentration of groundwater has increased, however, the Cl^-
550 concentrations have not, and in some areas have decreased. The major change has been large
551 increases in SO_4^{2-} and NO_3^- concentrations, which have increased several times compared to
552 1981. This indicates that the local government efforts to restrict groundwater abstraction have

553 been effective in their purpose of limiting saline intrusion; however, water quality
554 degradation has continued due to a new source- nitrate and sulphate contamination, largely
555 resulting from the heavy application of agricultural fertilizers.

556 There are the increasing trends of $\delta^{13}C_{DIC}$ and $\delta^{34}S_{SO4}$ values for groundwater along the
557 flow path. The enrichment of $\delta^{13}C_{DIC}$ of groundwater may be caused by kinetic isotope
558 effects as most groundwater is supersaturated with respect to calcite and dolomite, which can
559 cause $^{12}CO_2$ loss during exsolution and ^{13}C enrichment in solution. The pH and $\delta^{13}C$ values
560 of the investigated groundwater suggest evolution in a closed system. The potential sources
561 of dissolved SO_4^{2-} in the coastal aquifers include natural and artificial sulfates in rainwater,
562 dissolution of sulfate evaporates (e.g. gypsum and anhydrite), seawater, and anthropogenic
563 pollutants (e.g. agricultural fertilizers). We estimated the contributions of the four different
564 sources on the dissolved sulphate in groundwater quality by using mass balance approach.
565 Apart from seawater and precipitation (less than 10%), the fertilizer contribution in sulphate
566 concentrations of groundwater could be as high as an average of 62.1% in the Quaternary
567 aquifer, and 48.7% in the deeper carbonate aquifer, depending on the end-member
568 composition used. Although the processes that affect the groundwater quality and the
569 contribution to the dissolved sulfate of groundwater in the Daweijia area should be further
570 evaluated by more investigation (such as nitrogen isotope data), the current research results
571 obtained from a set of geochemical and isotopic tools show the sulfate contribution from

572 fertilizer application, compared with that from seawater intrusion and precipitation
573 infiltration, is dominant, with a secondary source from long-term evaporite dissolution and
574 de-dolomitization as water equilibrates with the carbonate aquifer matrix.

575 Also, there are similar ranges of NO_3^- concentrations, isotopic compositions ($\delta^{13}C_{DIC}$
576 and $\delta^{34}S_{SO4}$) and water type in the shallow Quaternary and deeper carbonate aquifers in most
577 parts of the study area, indicating interaction between shallow and deep groundwater in the
578 study area, which has implications for aquifer protection from contamination by agricultural
579 chemicals.

580 Coastal carbonate aquifers, a prolific groundwater source worldwide, are characterized
581 by rapid groundwater circulation and recharge and are therefore highly vulnerable to
582 anthropogenic contamination. Human activities in heavily populated areas such as the current
583 study are now potentially the key driver in the hydrology and hydrochemical evolution of
584 some of these coastal aquifers, as demonstrated here. Only by strictly controlling
585 anthropogenic land-use and water use activities can the pollution and degradation of these
586 aquifers be prevented. Future studies could focus on the seasonal variation of sulfur and
587 nitrogen isotopes of dissolved SO_4^{2-} and NO_3^-, respectively, and more detailed analysis of
588 these stable isotopes in soil profiles. This could provide more insight into the dynamics of
589 contamination of this and other similar aquifers.

Acknowledgements

This research was partially funded by Zhu Kezhen Outstanding Young Scholars Program (No.2015RC102), Institute of Geographic Sciences and Natural Resources Research, Chinese Academy of Sciences. It was undertaken as part of a groundwater survey project entitled "Assessment of Vulnerability and Investigation of Environmental Geology in the Key Section of Circum-Bohai-Sea Region". The authors are grateful to Dr. Yang Jilong, Dr. Liu Xin, Dr. Xie Hailan and Pan Tong for their help and support during water sampling and monitoring in the field and data collection. We also want to acknowledge the constructive suggestions from Prof. Ian Cartwright and another anonymous reviewer..

References

Appelo C.A.J., 1994. Cation and proton exchange, pH variations and carbonate recactions in a freshening aquifer. Water Resources Research, 30: 2793-2805.

Appelo C.A.J., Postma D., 2005. Geochemistry, groundwater and pollution, 2nd Edition: A.A. Balkema Publishers, Leiden, The Netherlands.

Aunay B., Dörfliger N., Duvail C., Grelot F., Le Strat P., Montginoul M., Rinaudo J.D., 2006. Hydro-socio-economic implications for water management strategies: the case of Roussillon coastal aquifer. In: International Symposium - DARCY 2006, Aquifer Systems Management, May 2006, Dijon, France. p9, 2006.

Back W., Hanshaw B.B., Pyle T.E., Plummer L.N., Weidie A.E., 1979. Geochemical significance of groundwater discharge and carbonate solution of the formation of Caleta Xel Ha, Quintana Roo, Mexico, Water Resour. Res., 15, 1521-1535, 1979.

Barlow P.M., Reichard E.G., 2010. Saltwater intrusion in coastal regions of North America. Hydrogeology Journal, 18: 247-260.

Cardenal J., Benavente J., Cruz-Sanjulián J.J., 1994. Chemical evolution of groundwater in Triassic gypsum-bearing carbonate aquifers (Las Alpujarras, southern Spain). Journal of Hydrology. 161:3-30.

Cartwright, I., Weaver, T.R., Fulton, S., Nichol, C., Reid, M., Cheng, X., 2004. Hydrogeochemical and isotopic constraints on the origins of dryland salinity, Murray Basin, Victoria, Australia. Applied Geochemistry 19, 1233-1254.

CGS (China Geology Survey), 2007. Assurance report of water supply in Dalian City. Geological survey institute of Liaoning Province, Dalian, China, 38-44, 2007.

Clark I., Fritz P., 1997. Environmental Isotopes in Hydrogeology. Lewis Publishers, Boca Raton.

621 Cravotta C.A., 1997. Use of Stable Isotopes of Carbon, Nitrogen, and Sulfur to Identify Sources of
622 Nitrogen in Surface Waters in the Lower Susquehanna River Basin, Pennsylvania. US Geol. Surv.
623 Water, Supply Paper, Denver, 2497, 1997.
624 Currell M.J, Han D.M, Chen Z.Y, Cartwright I., 2012. Sustainability of groundwater usage in northern
625 China: dependence on palaeowaters and effects on water quality, quantity and ecosystem health.
626 Hydrological Processes. 26: 4050-4066.
627 Currell M.J., Cartwright I., Bradley D.C., Han D.M., 2010. Recharge history and controls on groundwater
628 quality in the Yuncheng Basin, north China. Journal of Hydrology, 385: 216-229.
629 Daniele L., Vallejos Á., Corbella M., Luis Molina L., Pulido-Bosch A., 2013. Hydrogeochemistry and
630 geochemical simulations to assess water-rock interactions in complex carbonate aquifers: The case of
631 Aguadulce (SE Spain). Applied Geochemistry. 29:43-54.
632 de Louw P.G.B.,Eeman S., Oude Essink G.H.P., Vermue E., Post V.E.A., 2013. Rainwater lens dynamics
633 and mixing between infiltrating rainwater and upward saline groundwater seepage beneath a tile-
634 drained agricultural field. Journal of Hydrology. 501:133-145.
635 de Montety V., Radakovitch O., Vallet-Coulomb C., Blavoux B., Hermitte D., Valles V., 2008. Origin of
636 groundwater salinity and hydrogeochemical processes in a confined coastal aquifer: Case of the Rhône
637 delta (Southern France).Applied Geochemistry. 23:2337–2349.
638 Deines P., Langmuir D., 1974. Stable carbon isotope ratios and the existence of a gas phase in the
639 evolution of carbonate ground waters. Geochimica et Cosmochimica Acta, 38:1147-1164.
640 Drever, J.I., 1997. The Geochemistry of Natural Waters: Surface and Groundwater Environments.
641 Prentice-Hall, New Jersey, USA. 436 pp.
642 Edmunds, W.M., 1996. Bromine geochemistry of British groundwaters. Mineralogical Magazine, 60:275-
643 284.
644 Edmunds, W.M., Cook, J.M., Darling, W.G., Kinniburgh, D.G., Miles, D.L., 1987. Baseline geochemical
645 conditions in the chalk aquifer, Berkshire, UK: a basis for groundwater quality management. Appl.
646 Geochem. 2:251-274.
647 Fan J.J., 1984. Seawater intrusion and calculation of groundwater exploitation in the karst area of the west
648 JinXian, Dalian. Hydrogeology & Engineering Geology (in Chinese with English abstract). 1:3-6.
649 Freeze, R.A. and Cherry, J.A., 1979. Groundwater. Prentice Hall, Englewood Cliffs, NJ, 604 pp.
650 Ghassemi F., Jakeman AJ., Nix HA., 1995. Salinisation of land and water resources: human causes, extent,
651 management and case studies. University of New South Wales Press, Sydney, 526 pp.
652 Ghiglieri G., Carletti A., Pittalis D., 2012. Analysis of salinization processes in the coastal carbonate
653 aquifer of Porto Torres (NW Sardinia, Italy). Journal of Hydrology. 432-433:43-51.
654 Giménez-Forcada E., 2010. Dynamic of sea water interface using hydrochemical facies evolution diagram.
655 Ground Water. 48(2):212-216.
656 Guo Y.H., Shen Z.L., Zhong Z.X., 1995. Downward movement of shallow saline groundwater and its
657 impact on deep-lying groundwater system. Hydrogeology and Engineering Geology (in Chinese with
658 English abstract). 2:8-12.

659 Halas S., Szaran J., 1999. Low-temperature thermal decomposition of sulfates to SO_2 for on-line $^{34}S/^{32}S$
660 analysis. Analytical Chemistry. 71: 3254-3257.
661 Han D.M., Kohfahl C., Song X.F., Xiao G.Q., Yang J.L., 2011. Geochemical and isotopic evidence for
662 palaeo-seawater intrusion into the south coast aquifer of Laizhou Bay, China. Applied Geochemistry,
663 26(5):863-883.
664 Han D.M., Post V.E.A., Song X.F., 2015. Groundwater salinization processes and reversibility of seawater
665 intrusion in coastal carbonate aquifers. Journal of Hydrology. 531(3): 1067-1080.
666 Hong Y.T., Zhang H.B., Zhu Y.X., Pu H.C., Jiang H.B., Liu D.P., 1994. Characteristics of sulfur isotope
667 composition of precipitation in China. Advances in Natural Sciences (in Chinese). 6(4):741-745.
668 Hosono T., Nakano T., Iget A., Tayasu I., Tanaka T., Yachi S., 2007. Impact of fertilizer on a small
669 watershed of Lake Biwa: Use of sulfur and strontium isotopes in environmental diagnosis. Science of
670 the Total Environment. 384:342-354.
671 Hu T., 2010. Analysis on economic benefit of Dalian suburban farming. Chinese agricultural science
672 bulletin (in Chinese with English abstract).26(17):393-397.
673 Hunkeler D., Mudry J., 2007. Hydrochemical methods. in Methods in karst hydrogeology:IAH
674 international contributions to hydrogeology (edited by Goldscheider N., Drew D.). British Geological
675 Survey, Wallingford, UK. Taylor & Francis Group e-Library, London, UK, pp99.
676 Jin Y.J., Wu Q., 1990. The application of the electrical logging of well fluid in determining the vertical
677 heterogeneity of sea water intrusion. Journal of Heibei College of Geology (in Chinese with English
678 abstract). 13(1):69-73.
679 Jones, B., Pleydell, S.M., Ng, K.-C., Longstaffe, F.J., 1989. Formation of poikilotopic calcite–dolomite
680 fabrics in the Oligocene–Miocene Bluff formation of Grand Cayman, British West Indies. Bull. Can.
681 Petrol. Geol. 37, 255-265.
682 Kaown D., Koh D-C., Mayer B., Lee K-K., 2009. Identification of nitrate and sulphate sources in
683 groundwater using dual stable isotope approaches for an agricultural area with different land use
684 (Chuncheon, mid-eastern Korea). Agriculture, Ecosystems and Environment, 132: 223-231.
685 Kim H., Kaown D., Mayer B., Lee J., Hyun Y., Lee K., 2015. Identifying the sources of nitrate
686 contamination of groundwater in an agricultural area (Haean basin, Korea) using isotope and microbial
687 community analyses. Science of the Total Environment. 533:566-575.
688 Kloppmann, W., Dever, L., Edmunds, W.M., 1998. Residence time of chalk groundwaters in the Paris
689 Basin and the North German Basin: a geochemical approach. Appl. Geochem. 13:593-606.
690 Kumar M., Rao M.S., Deka J.P., Ramanathan AL., Kumar B., 2015. Integrated hydrogeochemical, isotopic
691 and geomorphological depiction of the groundwater salinization in the aquifer system of Delhi, India.
692 Journal of Asian Earth Sciences.111:936-947.
693 Langmuir D., 1971. The geochemsitry of some carbonate ground waters in central Pennsylvania.
694 Geochimica et Cosmochimica Acta. 35:1023-1045.

695 Li, X.D., Harue, M., Kusakabe, M., Yanagisawa, F., Zeng, H.A., 2006. Degradation of groundwater
696 quality due to anthropogenic sulfur and nitrogen contamination in the Sichuan Basin, China. Geochem.
697 J. 40, 309-332.
698 López-Chicano, M., Bouamama, M., Vallejos, A., Pulido-Bosch, A., 2001. Factors which determine the
699 hydrogeochemical behavior of karst springs. A case study from the Betic Cordilleras, Spain. Appl.
700 Geochem. 16, 1179-1192.
701 Lü G., Zhao L.B., Sun X.Z., Tan D.F., 1981. Periodic summary report on investigating the environmental
702 hydrogeology in Dalian area (in Chinese). The Second Institute of hydrogeology and engineering
703 geology, Liaoning Bureau of Geology, Dalian, China, 48-66, 1981 (in Chinese).
704 McCaffrey, M.A., Lazar, B., Holland, H.D., 1987. The evaporation path of seawater and the
705 coprecipitation of Br^- and K^+ with halite. Journal of Sedimentary Petrology 57, 928-937.
706 Moral F., Cruz-Sanjulian J.J., Olias M., 2008. Geochemical evolution of groundwater in the carbonate
707 aquifers of Sierra de Segura (Betic Cordillera, southern Spain). J.Hydrol. 360, 281-296.
708 Myshakin E., Siriwardane H., Hulcher C., Lindner E., Sams N., King S., McKoy M., 2015. Numerical
709 simulations of vertical growth of hydraulic fractures and brine migration in geological formations
710 above the Marcellus shale. Journal of Natural Gas Science and Engineering. 27(2):531-544.
711 Najib S., Fadili A., Mehdi K., Riss J., Makan A., Guessir H.,2016.Salinization process and coastal
712 groundwater quality in Chaouia, Morocco. Journal of African Earth Sciences,115:17-31.
713 Otero, N., Canals, A., Soler, A., 2007. Using dual-isotope data to trace the origin and processes of
714 dissolved sulphate: a case study in Calders stream (Llobregat basin, Spain). Aquat. Geochem. 13, 109-
715 126.
716 Parkhurst D.L., Appelo C.A.J., 1999. User's Guide to PHREEQC-A Computer Program for Speciation,
717 Reaction-Path, 1D-Transport, and Inverse Geochemical Calculation, US Geol. Surv. Water-Resour.
718 Invest. Rep., US Geol. Surv., Denver, Colorado, 99-4259, 1999.
719 Plummer L.N., Busby J.F., Lee R.W., Hanshaw B.B., 1990. Geochemical modeling in the Madison aquifer
720 in parts of Montana, Wyoming and South Dakota. Water Resour. Res. 26, 1981-2014.
721 Plummer L.N., Sprinkle C.L., 2001. Radiocarbon dating of dissolved inorganic carbon in groundwater
722 from confined parts of the Upper Floridan Aquifer, Florida, USA. Hydrogeol. J. 9, 127-150.
723 Rees C.E., 1978. The sulphur isotopic composition of ocean water sulphate. Geochimica et Cosmochimica
724 Acta. 42(4):377-381.
725 Sánchez-Martos F., Pulido-Bosch A., Molina-Sánchez L., Vallejos-Izquierdo A., 2002. Identification of
726 the origin of salinization in groundwater using minor ions (Lower Andarax, Southeast Spain). The
727 Science of the Total Environment. 297:43-58.
728 Schiavo M.A., Hauser S., Povinec P.P., 2009. Stable isotopes of water as a tool to study groundwater–
729 seawater interactions in coastal south-eastern Sicily. Journal of Hydrology. 364(1-2):40-69.
730 Shi Z.S., Chen K.Y., Shi J., He H.J., Liu B.J., 2004. Sulfur isotopic composition and its geological
731 significance of the Paleogene sulfate rock deposited in Dongpu Depression. Petrol. Explor. Develop (in
732 Chinese). 31 (6):44-46.

733 Song Q.C., 2013. Status quo of seawater intrusion in Daweijia karst water source of Dalian, China. Journal
734 of Chengdu University of Technology (Science & Technology Edition) (In Chinese with English
735 abstract). 40(3): 348-352.
736 Szynkiewicz A., Newton B.T., Timmons S.S., Borrok D.M., 2012. The sources and budget for dissolved
737 sulfate in a fractured carbonate aquifer, southern Sacramento Mountains, New Mexico, USA. Applied
738 Geochemistry. 27:1451-1462.
739 Szynkiewicz A., Witcher J.C., Modelska M., Borrok D.M., Pratt L.M., 2011. Anthropogenic sulfate loads
740 in the Rio Grande, New Mexico (USA). Chemical Geology.283(3-4):194-209.
741 Unland N.P., Taylor H.L., Bolton B.R., Cartwright I., 2012. Assessing the hydrogeochemical impact and
742 distribution of acid sulphate soils, Heart Morass, West Gippsland, Victoria. Applied Geochemistry.
743 27(10):2001-2009.
744 Vitòria L., Otero N., Soler A., Canals À., 2004. Fertilizer characterization: Isotopic Data (N, S, O, C, and
745 Sr). Environ. Sci.Technol. 38:3254-3262.
746 Vogel J.C., 1993. Variability of carbon isotope fractionation during photosynthesis. In: J.R.Ehleringer, A.E.
747 Hall and G.D. Farquhar (Eds.) Stable Isotopes and Plant Carbon –Water Relations, Academic Press,
748 San Diego, CA: 29-38.
749 Wu Q., Jin Y.J., 1990. Characteristics of seawater intrusion in coastal karst groundwater system of
750 Daweijia area, Dalian City. Geotechnical Investigation & Surveying (In Chinese with English abstract).
751 3:43-44.
752 Wu Q., Jin Y.J., Li D.A., Xia Y.H., 1994. The mechanisms of seawater intrusion of karst groundwater
753 system in Daweijia, Dalian City and the countermeasures of its control. The Chinese Journal of
754 Geological Hazard and Control (in Chinese with English abstract).1:64-68.
755 Yang J.L., 2011. Hydrogeochemical reactions in seawater intrusion process in Daweijia water source area，
756 Dalian City (In Chinese with English abstract). Master's degree thesis, Jilin University (Changchun,
757 China). pp14-15.
758 Zhang X.Y., Jiang H., Zhang Q.X., Zhang X., 2012. Chemical characteristics of rainwater in northeast
759 China, a case study of Dalian. Atmospheric Research 116:151-160.
760 Zhao C.R., Yang J.L., Xiao G.Q., Du D., Pan T., Zhang S.F., 2012. Hydrogeochemical reactions and
761 hydrogeological model for seawater intrusion processes in the Daweijia water source area，Dalian City.
762 Geological Survey and Research (in Chinese with English abstract). 35(2):154-160.
763 Zhao T.S., 1991. Problems of karst groundwater development in littoral area and its ultimate control
764 method. The Chinese Journal of Geological Hazard and Control (in Chinese with English abstract),
765 4:73-77.
766
767
768
769
770

FIGURES:

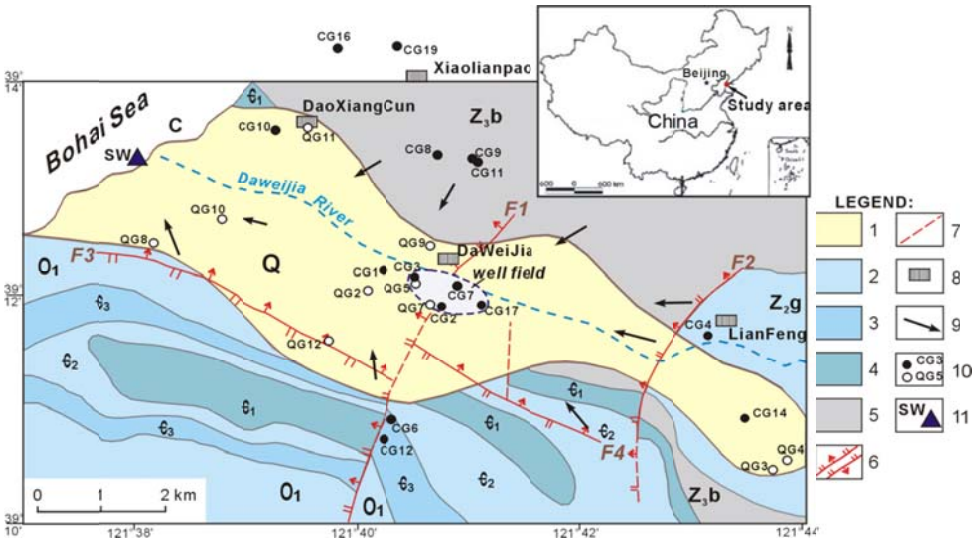

Fig. 1. Geological setting and water sampling locations. Geology modified after Wu and Jin (1990). Formation note: O_1- Lower Ordovician; ϵ_3-Upper Cambrian; ϵ_2-Middle Cambrian; ϵ_1-Lower Cambrian;Z_2g-Ganjingzi group of Middle Sinian; Z_3b- Beishan group of Upper Sinian. Legend: 1-Quaternary sediments; 2-thick-beded limestone; 3-laminated limestone with shale; 4-argillaceous limestone; 5-sandstone and shale; 6- normal/thrust fault; 7- buried fault; 8- town location; 9- approximate groundwater flow direction; 10-sampling wells ●from deep carbonate aquifers (depth>80 m), ○ from shallow Quaternary aquifer (depth<40 m); 11-sampling site for seawater.

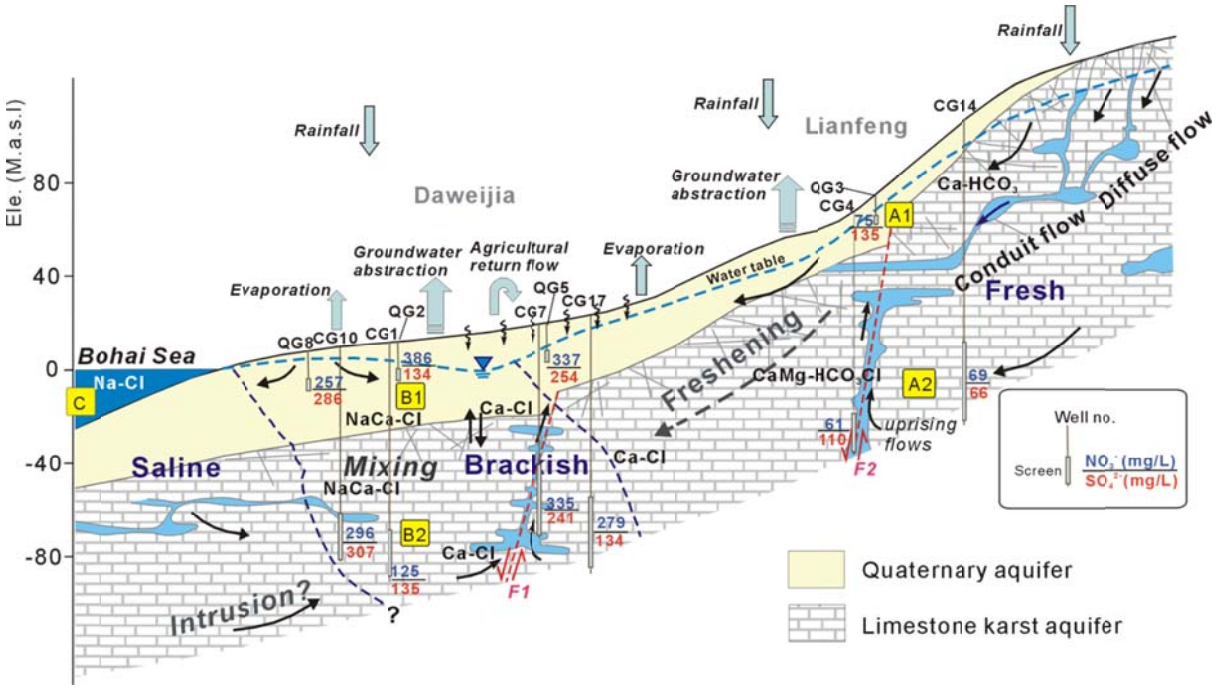

Fig. 2. Conceptual model showing the hydrogeological system (modified after Yang, 2011) and NO_3^- and SO_4^{2-} concentrations and sources. Characteristic ranges of $\delta^{13}C$ and $\delta^{34}S_{SO4}$ values for A1, A2, B1, B2 and C are shown in Table 3. Arrows in aquifers indicate general groundwater flow direction.

802

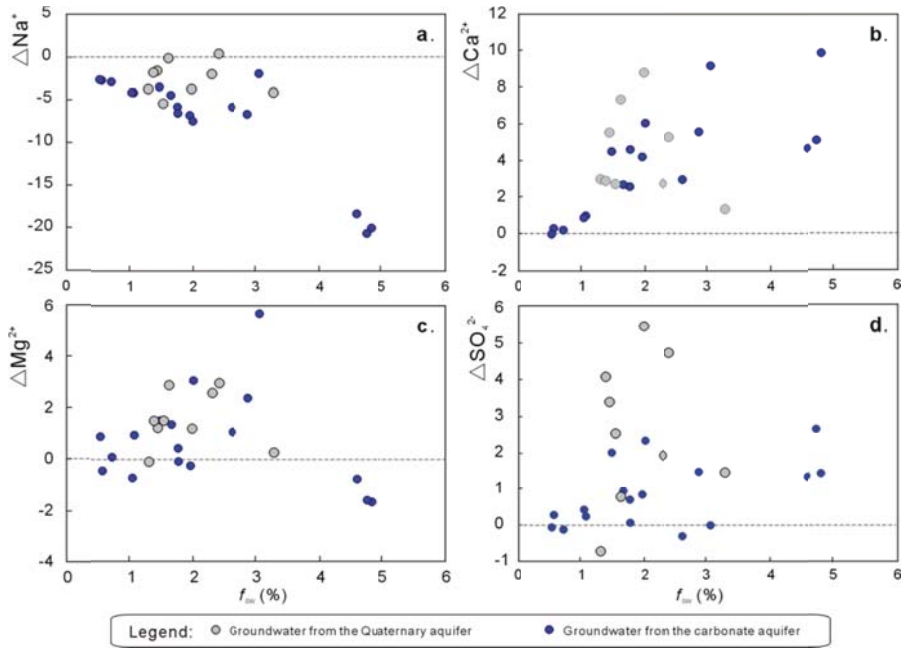

803

804 Fig. 3. Graphs showing the cationic Δ-values of groundwater samples vs. fraction of seawater:

805 (**a**) ΔNa^{+}; (**b**) ΔCa^{2+}, (**c**) ΔMg^{2+}, and (**d**) ΔSO_4^{2-}.

806

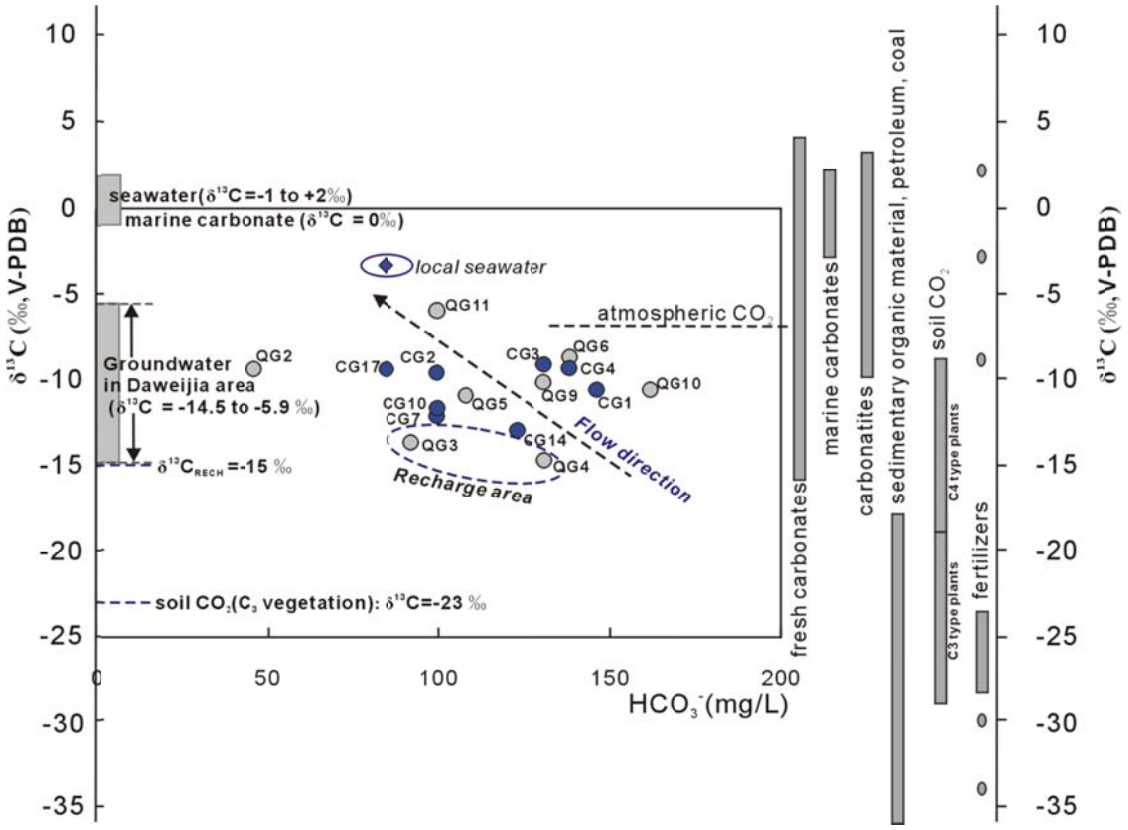

807

808 Fig. 4. $\delta^{13}C_{DIC}$ vs. dissolved inorganic carbon for the groundwater samples (Aug.2009) in the

809 Daweijia area, comparing with $\delta^{13}C$ values for the main carbon reservoirs (Vitòria et al., 2004

810 and therein). See Fig. 3 for legend.

811

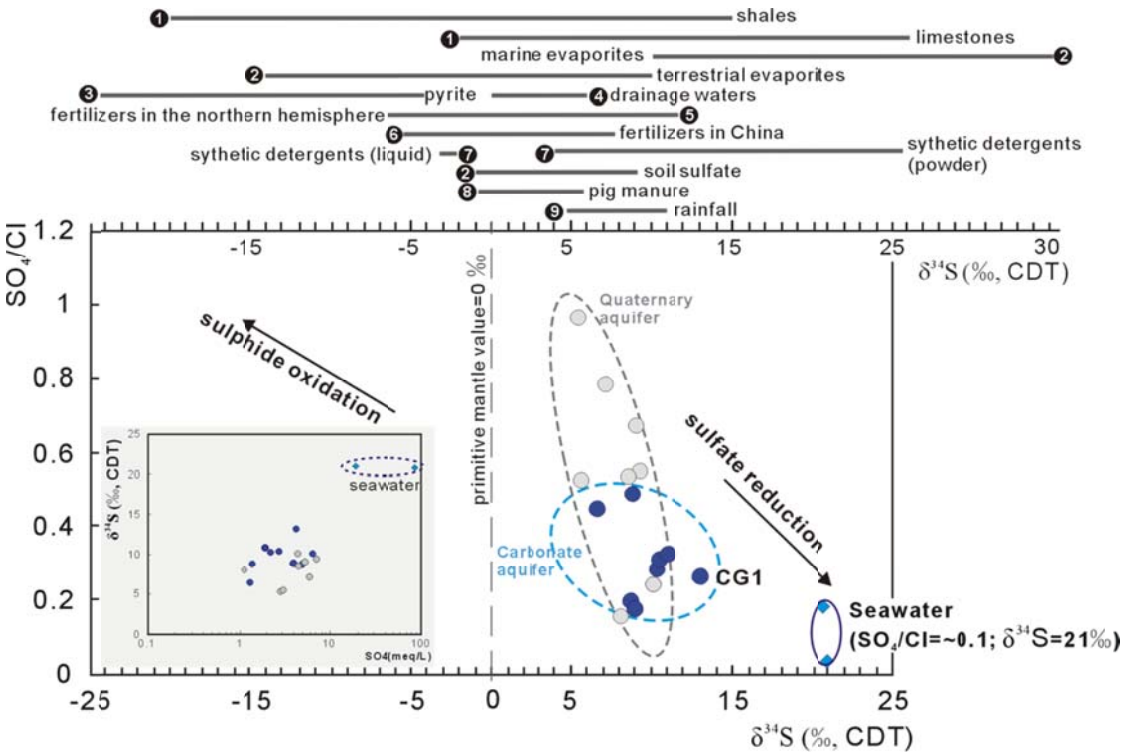

812

813 Fig. 5. $\delta^{34}S$ of dissolved SO_4 versus SO_4/Cl for groundwater samples from the Daweijia area

814 The range of sulfur isotopic values of some major sulfur reservoirs and selected materials is summarized from literature
815 compiled data as follows: 1-Clark and Fritz, 1997; 2- Vitòria et al., 2004; 3- Szynkiewicz et al., 2012; 4- Unland et al., 2012;
816 5- Szynkiewicz et al., 2011; 6- Li et al., 2006; 7- Hosono et al., 2007; 8- Cravotta, 1997 and Otero et al., 2007; 9- Hong et al.,
817 1994. See Fig. 3 for legend.

818

819

820

821

822

823

824

825

826

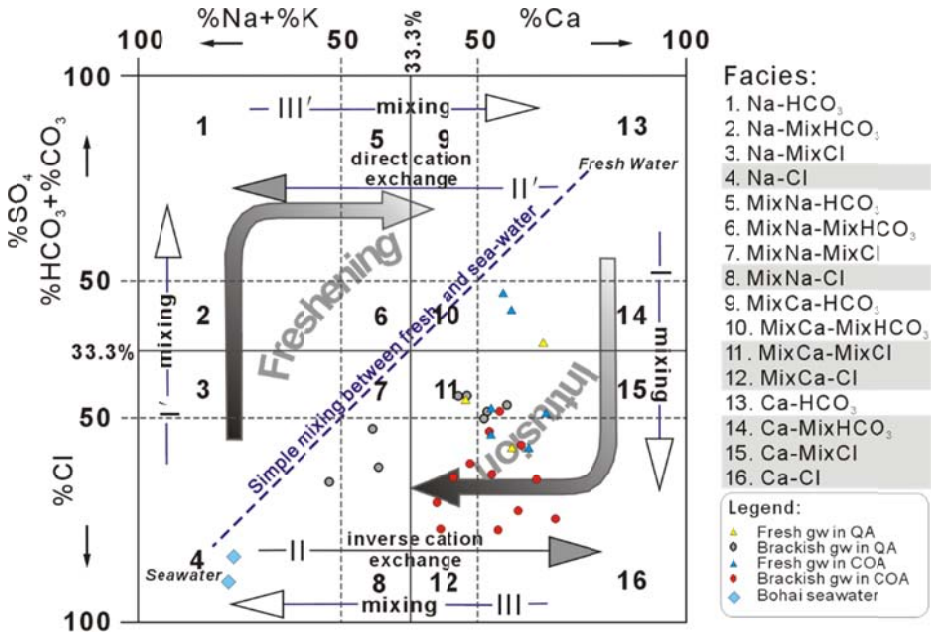

827

828 Fig. 6. Hydrogeochemical Facies Evolution (HFE) diagram.

829 QA-Quaternary aquifer; COA- Cambrian- Ordovician carbonate aquifer.

830

831

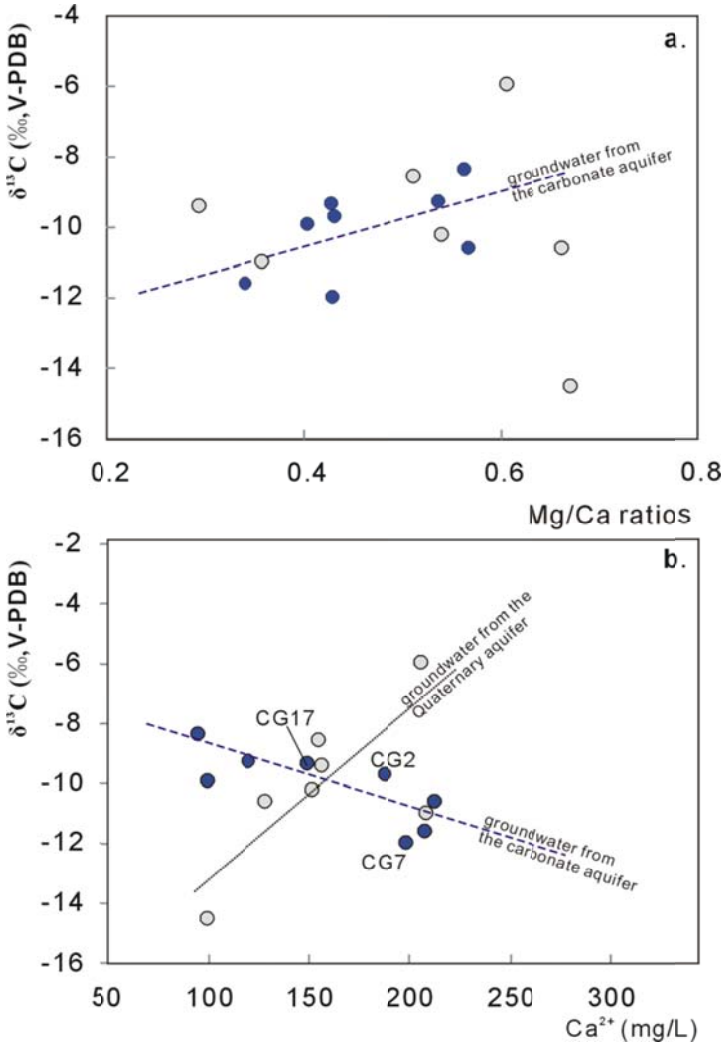

Fig. 7. Graphs showing (a) Mg/Ca ratios (by meq/L); (b) Ca^{2+} concentrations vs. $\delta^{13}C_{DIC}$ values in different aquifers (grey- groundwater samples collected from the Quaternary aquifer; blue- groundwater samples collected from the carbonate aquifer). See Fig. 3 for legend.

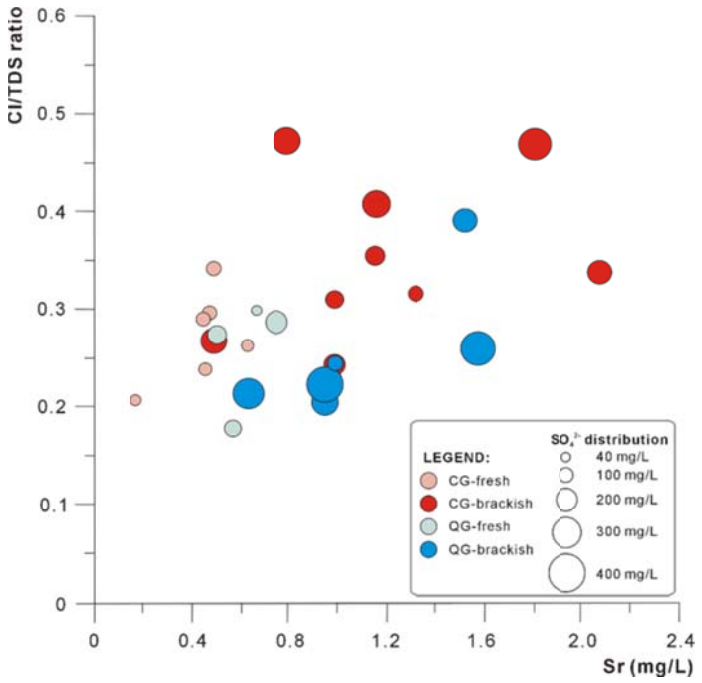

Fig. 8. Plot of Cl/TDS ratio vs. Sr (mg/L) from groundwater samples in the Daweijia area. Sulphate concentration of each sample is also indicated by the size of the point. CG-groundwater from carbonate aquifer; QG-groundwater from Quaternary aquifer.

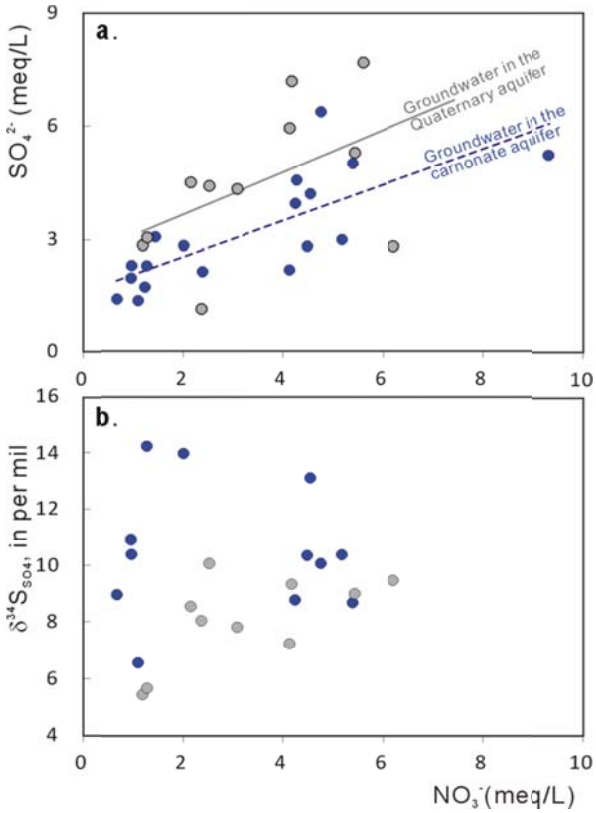

Fig. 9. Bivariate plots for **a** relationship **b**etween SO_4^{2-} and NO_3^- concentration and **b** $\delta^{34}S_{SO4}$ vs. NO_3^- concentrations. See Fig. 2 for legend.

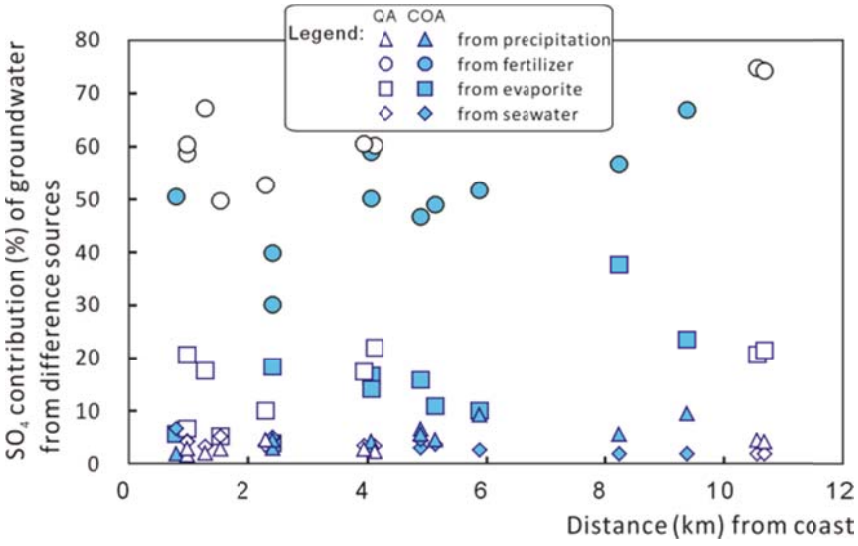

Fig. 10. Calculated SO_4^{2-} contribution of groundwater from four different sources (QA-groundwater from the Quaternary aquifer; COA-groundwater from the carbonate aquifer)

863 Table 1 Hydrochemical and isotopic data of the June 2006(*) and August 2010 field sampling

Sample	Well Depth (m)	Screened Intervals (m)	EC (μs/cm)	pH	T (°C)	ORP (mV)	DO (mg/L)	Ca^{2+} (mg/L)	Na^{+} (mg/L)	K^{+} (mg/L)	Mg^{2+} (mg/L)	Cl^{-} (mg/L)	SO_4^{2-} (mg/L)	NO_3^{-} (mg/L)	HCO_3^{-} (mg/L)	Sr (mg/L)	SI_{cal}	SI_{dol}	SI_{gyp}	$\delta^{34}S_{SO4}$ (‰)	$\delta^{13}C_{DIC}$ (‰)
Groundwater samples collected from the carbonate aquifer:																					
CG4	100	70-95	1015	7.2	16.1	193	3.6	119.6	50.5	1.2	38.5	261.0	109.7	60.9	247.1	0.49	0.1	-0.07	-1.47	10.4	-9.3
CG16	88	58-84	715	7.5	22.4	2	5.7	100.9	26.1	4.7	16.1	112.1	82.4	77.2	101.2	0.45	0.1	-0.24	-1.58		
CG3	110	72-98	986	7.3	19.3	201	4.0	115.8	47.2	1.5	37.8	209.5	93.8	60.3	282.8	0.47	0.27	0.33	-1.55	10.9	
CG6	120	75-112	796	7.3	21.7	139	3.7	99.4	38.2	1.2	24.1	141.6	67.1	43.1	250.1	0.63	0.23	0.18	-1.41	9.0	-9.9
CG14	128	85-118	749	7.6	22.0	34	7.2	94.5	24.5	1.0	31.9	105.7	65.1	69.1	238.1	0.17	0.48	0.84	-1.75	6.6	-8.4
CG9	100	68-92	846	7.6	18.8	2	8.6	113.6	44.4	6.5	17.4	203.8	101.8	147.9	134.0	0.45	0.21	-0.14	-1.47		
CG2	120	72-107	2050	6.5	16.0	186	7.5	187.7	106.0	2.3	48.5	288.4	189.2	263.9	199.4	0.99	-0.59	-1.53	-1.12	8.8	-9.7
CG7	92	59-88	1761	6.6	17.0	222	6.6	198.5	97.8	1.0	51.1	892.9	240.5	334.7	145.9	0.79	-0.65	-1.65	-1.05	8.7	-12.0
CG17	110	68-97	1370	7.0	14.2	200	7.0	149.1	82.9	1.5	38.3	343.4	134.1	278.8	163.7	0.99	-0.31	-1.01	-1.31	10.4	-9.3
CG1	100	71-93	2280	7.2	18.2	163	5.6	212.5	184.0	3.5	72.3	561.0	201.4	282.6	282.8	2.07	0.27	0.32	-1.12	13.1	-10.6
CG8	95	65-92	1416	7.4	20.0	199	6.1	190.6	66.7	1.4	32.1	344.5	104.1	256.6	190.5	1.32	0.38	0.27	-1.35		
CG11	100	67-93	2050	7.1	15.1	2	7.6	302.8	84.3	1.7	42.3	937.3	249.9	579.4	205.4	1.16	0.14	-0.36	-0.9		
CG12	100	68-93	1362	7.3	20.0	25	7.4	183.0	81.3	1.6	31.9	380.8	146.2	90.1	318.5	1.15	0.51	0.55	-1.24		
CG19	62	43-59	1481	6.7	14.5	26	4.7	220.0	70.6	2.0	72.1	390.0	219.1	265.6	446.5	0.49	0	-0.28	-1.05		
CG10	90	59-86	1586	7.4	21.5	214	7.4	207.7	62.0	26.4	42.4	923.5	306.9	295.7	205.4	1.80	0.35	0.31	-0.95	10.1	-11.6
CG1*	100	71-93	2890	7.3	14.9			284.5	312.2	3.7	114.0	596.6	135.3	124.8	253.8	-	0.34	0.5	-1.23	14.0	
CG2*	120	72-107	2110	7.0	13.2			151.2	103.2	1.5	48.4	323.3	142.7	321.5	174.2	-	-0.33	-0.97	-1.29	10.4	
CG3*	110	72-98	2300	7.2	13.2			158.9	175.6	3.5	54.2	511.2	109.4	79.6	120.8	-	-0.28	-0.85	-1.41	14.2	
Groundwater samples collected from the Quaternary aquifer:																					
QG7	28	15-24	1242	7.6	13.1	2	6.7	156.2	82.1	1.0	27.5	254.5	54.4	146.6	262.0	0.66	0.56	0.55	-1.65	8.1	-9.4
QG3	8.4	6-7.5	821	7.0	18.3	52	4.4	118.3	28.6	4.0	21.6	103.3	135.4	74.7	190.5	0.57	-0.24	-0.95	-1.34	5.4	-12.8
QG4	14	7-13	912	7.5	23.0	22	3.6	99.1	42.5	13.1	40.0	203.3	145.2	80.2	241.1	0.50	0.34	0.6	-1.43	5.7	-14.5
QG5	12	7-11	1903	7.0	17.1	219	3.6	208.4	146.0	0.5	44.7	281.3	254.3	337.3	199.4	0.95	-0.03	-0.48	-0.98	9.0	-11.0
QG10	10	6-9	2210	7.2	13.9	204	5.0	128.2	286.1	12.8	51.0	640.6	211.5	156.1	309.6	1.52	0.04	-0.13	-1.27	10.1	-10.6
QG8	15	9-14	1633	7.4	16.4	16	7.8	154.6	134.5	2.7	47.5	269.8	285.9	256.9	220.3	0.63	0.31	0.33	-1.03	7.2	-8.6
QG9	20	12-17	1289	7.3	20.7	23	4.4	151.4	67.8	7.6	49.1	299.4	216.2	133.5	241.1	0.75	0.27	0.34	-1.15	8.6	-10.2
QG11	17	8-15	2780	7.4	23.2	65	1.3	205.8	295.5	11.1	74.8	469.4	344.9	259.5	291.7	1.58	0.59	1.07	-0.95	9.4	-5.9
QG12	17	12-16	2210	7.0	14.2	41	5.6	274.7	154.6	2.3	49.6	386.2	368.8	347.9	300.7	0.95	0.19	-0.16	-0.76		
QG2*	22	15-21	2310	7.0	15.2			244.9	198.5	3.6	66.3	315.7	134.2	386.3	512.7	-	0.32	0.29	-1.23	9.5	
QG11*	17	8-15	2820	7.2	13.9			153.8	229.2	4.4	69.2	448.3	207.6	190.6	200.9	-	-0.1	-0.35	-1.19	7.8	
SW1	Seawater sample		43800	7.7	26.8	171	5.0	324.5	7626.0	289.1	978.8	16683.9	4116.0	1092.0	163.7	5.81				20.8	-3.3

Table 2 – Summary of main hydrochemical processes occurring in the carbonate and quaternary aquifer, along with evidence used to assess the process

Aquifer (Carb/Quat)	Process	Occurring (Y/N)?	Evidence (1)	Evidence (2)	Figure
Carbonate Aquifer	Calcite dissolution (congruent)	No	Most groundwater samples with $SI_{calcite}$<0.1 and Ca:HCO_3 >1:2	No correlation between Ca or HCO_3 and $\delta^{13}C$	Figure 7
	Incongruent dolomite weathering	Yes	Increase in Mg/Ca along the flow path	Increase in $\delta^{13}C$ with increasing Mg/Ca	Figure 7a
	Cation exchange	Yes	Most samples with negative ΔNa^{+} values and positive ΔCa^{2+} + ΔMg^{2+} values	MixCa-Cl facies in HFE diagram	Figure 3; Figure 6
	Fertilizer addition	Yes	Positive correlation between NO_3^- and SO_4^{2-} concentrations	Mass balance results from different sources of $\delta^{34}S_{SO4}$	Figure 9 Figure 10
	Gypsum dissolution	Yes	All water samples with SI_{gypsum}<-0.5	Ca/SO_4 ratios >1	-
Quaternary Aquifer	Calcite dissolution (congruent)	Minor	Lack of correlation between $\delta^{13}C$ and HCO_3; Increasing $\delta^{13}C$ with increasing Ca	Most groundwater samples with $SI_{calcite}$<0.1 and Ca:HCO_3 around 1:2	Figure 7
	Incongruent dolomite weathering	No (apart from QG3)	$SI_{dolomite}$>-0.5; Mg:HCO_3>1:4	No obvious increasing trend in $\delta^{13}C$ with increasing Mg/Ca	Figure 7
	Cation exchange	Yes	Enrichment in Ca and loss of Na along flow path	$SI_{calcite}$ and $SI_{dolomite}$ close to or exceeding 0	Figure 3
	Addition of sulphate from fertilizer	Yes	Positive relationship between SO_4 and NO_3	Increasing $\delta^{34}S$ values with increasing NO_3 concentrations	Figure 9 Figure 10
	Gypsum dissolution	Yes	Ca:SO_4 close to 1	SI_{gyp}<-0.5	-

881 Table 3 –Characteristic ranges of $\delta^{13}C$ and $\delta^{34}S_{SO4}$ values in groundwater and seawater (showing a vertically increasing trend) (see locations on Figure 2)

	Shallow groundwater from upperstream area (A1)	Deep groundwater from upperstream area (A2)	Shallow groundwater from downstream area (B1)	Deep groundwater from downstream area (B2)	Seawater (C)
$\delta^{13}C$(‰,V-PDB)	-14.5 ~ -13.5	-12.8 ~ -9.0	-11.0 ~ -5.9	-9.7 ~ -10.6	-1 ~ +2
$\delta^{34}S_{SO4}$ (‰,CDT)	5.4 ~ 5.7	9.0 ~ 10.9	7.2 ~ 10.1	8.7 ~ 13.1	21

882